

Improved PPP performance in regional networks

Stefano Gandolfi¹ · Luca Tavasci¹ · Luca Poluzzi¹

Received: 15 April 2014 / Accepted: 19 April 2015 / Published online: 30 April 2015
© Springer-Verlag Berlin Heidelberg 2015

Abstract It has been demonstrated that precise point positioning (PPP) is a powerful tool in geodetic and geodynamic applications. As is known, it provides solutions in the reference system of the satellite orbits. We focus on the strategy to transform PPP solutions into the International Terrestrial Reference System (ITRS) by applying a set of local Helmert transformation parameters obtained from a regional network rather than using global parameters. In order to carry out this test, a regional network composed of 14 stations was analyzed using GIPSY-OASIS II software, over a period of 6 years. Two solutions differently aligned to the ITRS were compared in terms of accuracy, scattering, frequency content and local movements. One solution is aligned to IGB08 through the X-files provided by JPL, while the other is aligned to the European reference frame densification of IGB08 using customized regional X-files. Therefore, both are updated realizations of the ITRS. The test shows that a regional, instead of a global, alignment to the ITRS can significantly improve the repeatability of the solutions. A small improvement can also be found in terms of agreement with the regional densification of IGB08. The analysis of the signal content in the differently aligned time series allowed some differences to be found, in terms of both frequency and magnitude. These differences are mainly due to an evident common signal that is defined for the whole area and which is removed when using regional alignment. Finally, residual scattering was calculated after removing the modeled signals from each time series, which results in a scatter

being significantly smaller for the regional solution than for the global solution. In order to obtain these results, the choice of the reference stations is a major question and therefore discussed in detail.

Keywords Precise point positioning · GIPSY-OASIS II · Regional GNSS networks · ITRS · Time series analysis

Introduction

Positioning by means of global navigation satellite system (GNSS) is one of the most widely used techniques in monitoring reference frames, plate motion, landslides and structures and mapping. The use of this system can vary in terms of data processing strategies, which depend on the applications. For each objective, there is a different optimum reference frame to be considered. For example, the adoption of a local reference frame can be the best choice for monitoring structures, while, for plate motion studies, a global reference frame is preferable. Moreover, the definition of an accurate and stable global reference frame has been a main focus of the geodetic community for the last 20 years. The International Terrestrial Reference System (ITRS) is realized by means of a terrestrial reference frame, updated over time following newly available techniques and knowledge. Over recent years, the more reliable global reference frames were ITRF_{yyyy}, successively updated into IGS_{yy} and IGB_{yy} using GNSS techniques. At the present time, IGB08 is the latest frame realization available (Rebischung 2012). All these reference frames were realized through a list of the mean positions and velocities of a global network, together with their covariance matrix.

Other regional reference systems based on the ITRS have also been defined. In Europe, for instance, the

✉ Luca Tavasci
luca.tavasci2@unibo.it

¹ DICAM, School of Engineering and Architecture, University of Bologna, Viale Risorgimento 2, 40136 Bologna, Italy

European Terrestrial Reference System (ETRS) realized by the European Terrestrial Reference Frame (ETRF) (Altamimi and Boucher 2002) is the commonly adopted reference in many countries and used in their national geodetic networks. In Italy, ETRF2000 (epoch 2008.0) was adopted as the “new official national reference frame” in 2012 and is based on a densification network called *Rete Dinamica Nazionale* (RDN) (Barbarella et al. 2009), formed by 99 stations uniformly distributed along the Italian peninsula and in neighboring countries. RDN includes stations belonging to the European reference frame (EUREF) Permanent Network (EPN) (Bruyninx et al. 2001) and some International GNSS Service (IGS) stations. As for all the geodetic networks that constitute a regional densification of the reference frame, RDN has to be tied to the updated global reference frame. In particular, RDN daily solutions need first to be expressed in IGB08 before being transformed into ETRF2000, which is achieved through 14 official Helmert parameters (Boucher and Altamimi 2011).

During the past few years, precise point positioning (PPP) has achieved performance levels comparable to those obtainable through the differencing approach (Griffiths and Ray 2009; Bisnath and Gao 2009), especially for GNSS permanent stations. It is known that PPP produces solutions that are related to the reference frame of the orbits, which constitute, indeed, the only constraint to a reference frame. In order to move from this reference frame to others, the relative transformation parameters have to be computed and applied. This must be carried out by considering a set of fiducial sites defined in the desired reference frame.

The alignment of a regional network to a conventional global reference frame can be performed using the global network or a regional subset for the area under consideration. A comparison between the two different approaches was investigated by Legrand and Bruyninx (2009), and they concluded that a global network was preferable because the parameters derived from a regional network were too dependent on the choice of considered sites.

On the other hand, an alignment based on a small network close to the analyzed area is the best choice for local monitoring applications (Wang et al. 2014), avoiding most of the common signals of the reference frame, or mis-modeling. When evaluating the absolute movements of a regional network, a local alignment can lead to some loss of information (Freymueller 2009), but it may yet be a good choice if the aim is to realize a local densification of the reference frame.

A main topic is to evaluate the benefits gained from the strategy of transforming the solutions into a formally defined reference frame, achieved by applying regional

transformation parameters instead of global parameters. Nevertheless, the impact of this strategy on the suitability of GPS solutions in other applications, such as geodynamics, subsidence and structure and landslide monitoring, is discussed in terms of spectral frequency analysis and the correlations between the time series. In order to carry out this work, data derived from a subset of EPN, used to monitor RDN and covering a period of 6 years, were processed and analyzed. We used GIPSY-OASIS II version 6.2.1 developed by JPL (Webb and Zumberge 1997).

Keeping in mind the purpose of estimating the consistency with a reference frame, two parameters were identified and will be discussed. The first relates to the closeness of the solutions to the IGB08 reference frame. The second parameter relates to the scattering that defines the repeatability of the solutions. As reference frame, we have considered the latest EUREF densification of IGB08 (ftp://epncb.oma.be/epncb/station/coord/EPN/EPN_A_IGb08.SNX.Z), which is a recent realization of the ITRS in Europe (release name: EPN_A_IGb08_C1800). This European solution was adopted as the reference frame and used to evaluate the consistency of the different solutions.

Data set description

The network being analyzed is a subset of EPN used in the RDN alignment to the ITRS. The criteria adopted to select the stations are based on site positions, data quality and consistency. Applying these criteria, only EPN class A (Bruyninx et al. 2013) stations were taken into consideration and the resulting network was composed of 16 stations located in Italy and neighboring regions (Fig. 1). The choice of using EPN stations in addition to the IGS stations was decided by the need to have a sufficient number of well-distributed sites that could ensure high redundancy in the estimation of transformation parameters. This meant that it was not possible to use IGB08.snx directly as a reference, but rather EPN_A_IGb08.SNX, which is the updated EUREF densification of IGB08. For this work, 6 years of daily thirty-second data were processed for the period 2007–2012. Due to some issues with stations ROVE and LAMP, discussed below, the network actually used was composed of 14 stations.

Geophysical models and boundary conditions adopted for PPP GPS data processing

GPS data were processed with PPP using GIPSY-OASIS II version 6.1.2 software. By realizing customized scripts, it was possible to carry out complete and automatic GPS data processing. Similar to differenced GPS data processing, in

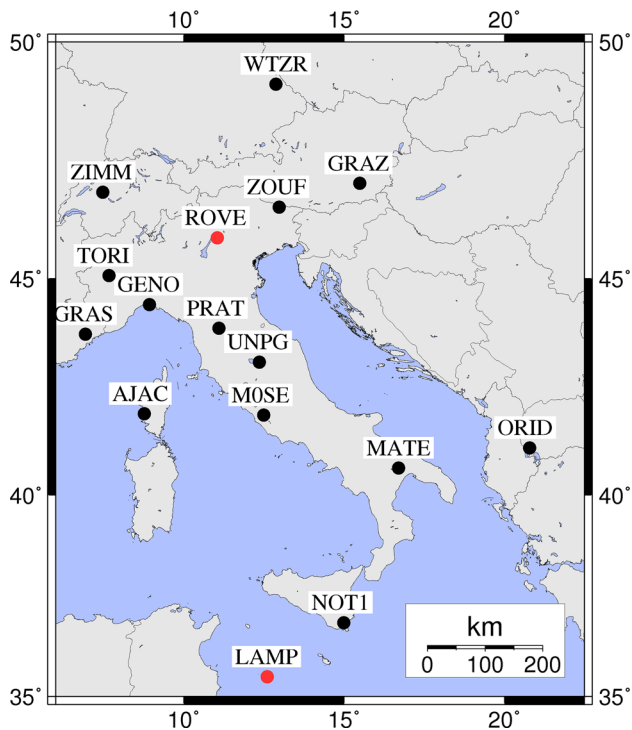


Fig. 1 Location of the 16 GNSS stations considered for the test. The 14 black dots represent the sites used to align the Italian National Network (RDN) to Igb08

a PPP approach, many parameters and boundary conditions must also be taken into account. These include geophysical models, antenna phase center calibration, cutoff angle for satellite observations, GPS ephemeris and ambiguity resolution. Below are the options selected for the test being discussed, most being the default parameters suggested by JPL for GIPSY users:

- Orbits and clocks products: non-fiducial precise FlinnR orbits from JPL, including information to enable the single receiver phase ambiguity resolution using GIPSY-OASIS software (WLPB) (Bertiger et al. 2010)
- Antenna phase center variation: IGS absolute phase center calibration file (igs08.atx)
- Cutoff angle for observations: 7°
- Tropospheric model: VMF-1 (Kouba 2008)
- Data rate: 300 s
- Smoother option: static solution.
- International reference ionosphere model: 2° order ionospheric model (Kedar et al. 2003)
- Number of iterations for the ambiguity resolution: 1
- Tide models: solid earth tide (WahrK1, FreqDepLove), polar tide model (PolTid) and ocean tide model (OctTid)—GIPSY default option
- Troposphere estimation parameters: random walk, set to 3 [mm/sqrt(h)] with wet gradient set to 3.6 [mm/h]—GIPSY default option

In the following, we will give the name “*native solution*” to the solution obtained directly from the GIPSY data processing procedure using JPL non-fiducial orbits and before any transformation into the ITRS.

Analysis of the “*native*” GIPSY solutions

For the *native* GIPSY solutions, the only constraint to a reference system is the non-fiducial FlinnR orbits adopted in the data processing, which are referred to a GPS-based reference system but adjusted to obtain the best self-consistency (Hurst 1995) and, therefore, not rigidly oriented in space. As an example, Fig. 2 shows two *native* solution time series for the WTZR and MATE stations with their mean motion removed and each referred to a local geodetic reference system. The mean motion was obtained using a linear regression based on a weighted least squares approach.

Figure 2 shows that the two series are quite highly correlated, even though the two stations are located at two completely different locations, about 980 km apart, and therefore cannot be influenced by such strong common effects. This same behavior is also noted when looking at the time series for every other pair of stations. The Pearson product-moment correlation coefficient ρ (Pearson 1895) was, therefore, calculated between the time series of a reference station and all the others. The correlation coefficient ρ_{rs} between two time series can be defined as:

$$\rho_{rs} = \frac{\sigma_{rs}}{\sigma_r \sigma_s} \quad (1)$$

where σ_r and σ_s represent the root-mean-square of the residuals to the regression line for the two time series, and σ_{rs} the relative covariance coefficient. The Pearson coefficient was computed between the WTZR station, which is the most northern one, and all the others, repeating this for each component, all expressed in a local geodetic reference frame (Table 1).

Table 1 highlights two main aspects: the high correlation for all the stations and the absence of a spatial dependence of the Pearson coefficients. This cannot be due to real spatially correlated effects, but must rather depend on the influences of the common environment and the impact of common boundary conditions, such as orbits, clocks and other remaining errors (Völksen 2005).

Strategies to align the PPP solutions to the ITRS: results and discussion

As was mentioned above, the transformation of the daily GPS solutions into the ITRS is necessary whenever there is a need to express the solution within a regional reference

Fig. 2 Comparison of two native GIPSY solutions time series for WTZR and MATE. Average velocities are there removed from each time series. The time series are expressed for each site in its local geodetic reference system. The *X-axis* represents the timescale in years, whereas the *Y-axis* represents the residual expressed in meters

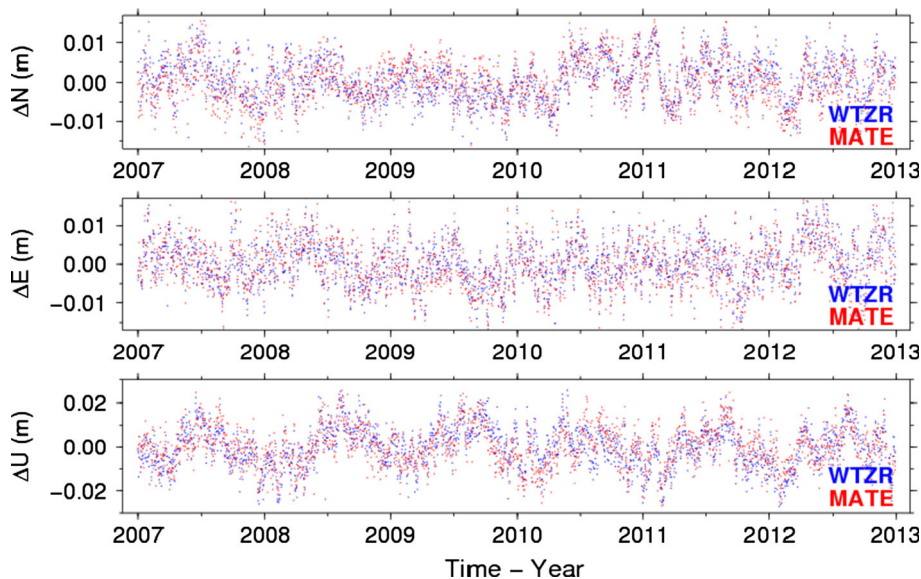


Table 1 Pearson’s correlation coefficients between the WTZR station and each of the others, expressed in the local geodetic components

Site	Correlation coefficient ρ_{rs}		
	N	E	U
AJAC	0.90	0.90	0.66
GENO	0.93	0.96	0.74
GRAS	0.91	0.94	0.76
GRAZ	0.94	0.96	0.84
LAMP	0.90	0.94	0.71
M0SE	0.93	0.95	0.77
MATE	0.89	0.95	0.76
NOT1	0.89	0.91	0.62
ORID	0.91	0.91	0.75
PRAT	0.70	0.95	0.56
ROVE	0.92	0.94	0.72
TORI	0.90	0.86	0.47
UNPG	0.91	0.94	0.75
ZIMM	0.93	0.95	0.80
ZOUF	0.91	0.94	0.81
Average value	0.90	0.93	0.71

Correlation coefficients are calculated from the time series of the residuals obtained subtracting the reference solution from the PPP solutions in order to remove the possible discontinuities, and then removing also the residual mean velocities

frame, such as ETRF2000 or RDN. In order to align the *native* GIPSY solutions (obtained using non-fiducial JPL products) to the ITRS, together with orbits and clocks, JPL also distributes what are known as X-files. These are daily files containing the seven Helmert parameters used to

transform each daily solution into the ITRS (IGS08 until 2012 DOY 280 and IGB08 from 2012 DOY 281). The parameters are calculated from a least squares method using the daily solutions of about 40 stations each day, selected by JPL from among about 200 IGS core network stations (Reischung et al. 2011). In this way, the JPL X-files were applied to the *native* solutions, obtaining a new time series for each station. This solution will be called the Global ITRS Solution (GIS).

A similar process can be applied to a local network. The GIPSY software package allows for the production of customized X-files, giving as input a set of daily solutions from the network and the corresponding reference solutions (*stacov2x* GIPSY script). Therefore, adopting the EPN_A_IGb08.SNX file as reference, a set of X-files was produced ad hoc for the analyzed network. For the method to function properly, a high number of stations must be considered in order to reach sufficient redundancy in the least squares approach. These transformation parameters were then applied to the *native* solution, obtaining another time series for each station. This solution will be called Regional ITRS Solution (RIS). GIS and the RIS are at the core of the following discussion and are two solutions for the same data set, differently aligned to the same reference frame, and so can be compared with the SINEX solution, even in terms of biases.

Focusing on the technical issues, where there is the need to be coherent with the chosen reference frame, the time series analysis discussed here is based on two statistical parameters. We define as “repeatability” the capability of obtaining similar results with several measurements and as “consistency” that of obtaining results close to the EPN_A_IGb08.SNX reference solution. Repeatability was

characterized by the scattering of the time series, whereas consistency by the biases to the reference solution. In spite of some natural causes that induce periodic movements to the station coordinates, the need to compare the results to a linearly defined reference solution imposes the evaluation of these parameters under the same linear approximation. Finally, in order to evaluate whether the use of regional parameters instead of global parameters leads to some loss of information, an analysis was performed in the frequency domain to evaluate the signal contents in both the GIS and RIS time series.

Statistical parameters and evaluation of the quality of the obtained solutions

In order to obtain the summary parameters needed to describe the behavior of the GNSS network solutions over a large lapse of time, in terms of both scattering and of biases, an automatic post-analysis procedure was implemented. First, the geocentric coordinates were transformed into a local geodetic reference system, to obtain results in terms of North, East and Up components, which can be interpreted easier. We assume $S_{kj}^i(t)$ as the value of the geodetic component (k) of a daily solution (j) of a GNSS station (i) at the epoch t , where $k = \text{North, East, Up}$, $j = 1, \dots, m$ with m number of daily solutions and $i = 1, \dots, n$ with n number of GNSS stations.

The consistency of the solutions is evaluated in terms of differences compared to the official EPN_A_IGb08.SNX solution for each station. To achieve this, the reference solution was converted to the same local geodetic system used for the S_{kj}^i solution, in order to evaluate the horizontal and the height components separately, and then the daily biases were calculated as:

$$\Delta_{kj}^i = S_{kj}^i - \text{REF}_{kj}^i \tag{2}$$

where REF_{kj}^i is the reference value of the k component. Therefore, Δ_{kj}^i can be considered as the residual between a daily GNSS solution and the official solution and together they generate the Δ_k^i time series which absorbs all the discontinuities in both the GNSS solutions and the SINEX file. For each time series, a linear regression was computed using a classical weighted least squares approach, with the weight being the inverse of the formal error derived by the data processing. We define m_k^i and q_k^i as the slope and the k -intercept of the linear regression, which we can now remove from the Δ_k^i time series by:

$$v_{kj}^i = \Delta_{kj}^i - [q_k^i + t(j) \times m_k^i] \tag{3}$$

where $t(j)$ is the time correspondent to the j -epoch. We can now define σ_k^i as the RMS of the residuals:

$$\sigma_k^i = \sqrt{\frac{1}{m} \sum_{j=1}^m v_{kj}^i{}^2} \tag{4}$$

In order to remove the outliers, an iterative procedure is adopted based on searching for the maximum outlier and then comparing it to the standard deviation. Daily coordinates are considered as outliers when:

$$\max\{|v_{kj}^i|\} > 3\sigma_k^i \tag{5}$$

The RMS σ_k^i is recalculated iteratively after each outlier rejection, specifying that for every outlier, even if just one component is involved, all the three components of that daily solution are removed. When no more outliers are found, the final parameter representing the repeatability of the time series is calculated as:

$$p_k^i = \sqrt{\frac{\sum_{j=1}^{m_{\text{clean}}} v_{kj}^i{}^2}{m_{\text{clean}}}} \tag{6}$$

where m_{clean} is the number of daily coordinates after the outlier rejection process. The solutions removed through these steps are also removed in Δ_k^i . As a representative parameter of the consistency of a time series with the reference solution, we calculate the following mean value of the biases:

$$b_k^i = \frac{\sum_{j=1}^{m_{\text{clean}}} \Delta_{kj}^i}{m_{\text{clean}}} \tag{7}$$

Finally, in order to summarize the above parameters of each series into a summary one for the whole network, for each reference component, we calculate two more parameters.

$$P_k = \frac{\sum_{i=1}^n P_k^i}{n} \tag{8}$$

$$B_k = \frac{\sum_{i=1}^n |b_k^i|}{n} \tag{9}$$

The first is P_k that represents the overall repeatability of the measures for the k component, while the second parameter B_k concerns the overall consistency with the reference solution.

Test results in terms of repeatability and accuracy

GIS and RIS were first compared to the EPN densification of the IGb08 reference solution in order to detect any misalignments. After this check, the stations LAMP and ROVE showed mean velocities significantly different than those of the reference, in both the GIS and the RIS. Since quite a high number of reference stations were available, these two sites were discarded and the regional

transformation parameters recalculated. All the results later discussed relate to the 14 stations composing the reference for RDN. Figure 3 shows the time series of the residuals with respect to the EPN densification of IGB08, for the 14 stations considered, with their regression lines, both for GIS (red dots) and for RIS (blue dots). It is evident that consistency with respect to the reference is high for both GIS and RIS, as almost all the solutions are within 5 mm from zero, including in height. No major discontinuity is evident in these time series, whereas some periodical signals clearly appear and will be discussed later. As expected, we observe that the time series are more scattered in the Up component than in the horizontal one and in some cases are evident that the RISs are less scattered than for the GISs.

Table 2 shows the test results for repeatability and consistency of both GIS and RIS. Regarding repeatability, a significant improvement is reached by using regional parameters, especially in the Up component, which is notoriously the weakest. The reduction in scattering is about 37 % for both horizontal and height components. The consistency of the GIS compared to the reference solution is already at the millimeter level when applying the global parameters, with the improvement of about 1 mm in the North component when regional parameters are applied. It is also important to underline that, at this level of analysis, all possible periodical signals defining each site have not yet been removed. These signals are considered as noise with respect to the linear motion of the sites assumed here, meaning that the obtained repeatability values should generally be higher than the real noise of the time series.

Pearson's correlation coefficients were then calculated for GIS and RIS, in the same way as for the native solution, and reported in Table 3. GIS reduces the correlation coefficient values from 0.90, 0.93 and 0.71 in the *native* solutions to 0.43, 0.53 and 0.43 for the North, East and Up components, respectively. As for the RIS, a strong overall decrease in these values toward -0.05 , -0.06 and -0.06 indicates that there is an almost complete decorrelation between all the time series. To complete this analysis, it is important to highlight that the number of outliers removed using the approach described above is virtually negligible. In particular, for GIS, the percentage of rejected solutions is between 0 and 1.7 %, whereas for RIS, they go from 0 to 3.7 %. The higher number of rejections in RIS is probably due to the lower values of σ_k^i for that solution.

Analysis in the frequency domain

Above we analyzed applications where consistency to a defined reference frame is the major topic. For other applications, such as geophysical studies, structures, landslides and ground subsidence monitoring, the absolute

position is not the main issue. In such applications, the goal of the positioning system is to allow a reliable interpretation of the local movement of the monitored point. For those applications, assuming linear motion in the definition of a reference frame is no longer an option since we need to model the point movement, including non-linear motion. As is well known (Dong et al. 2002; Mao et al. 1999), GNSS time series can be represented with a motion composed of a linear trend and many seasonal and periodical components. Moreover, most of the GNSS time series are spaced unequally over time because of interruptions in acquiring the observations. One of the well-known methods of performing spectral analysis on such series is based on the Lomb–Scargle periodogram (LSP) (Lomb 1976; Scargle 1982), coupled to the maximum likelihood estimation (MLE). With LSP, it is possible to evaluate the most probable periodical components and then calculate the amplitude and phase of these signals using MLE.

Starting from the residual series v_k^i (3), for each solution, we perform the Lomb–Scargle periodogram, allowing us to obtain the frequency power function. We then select the first five frequencies f_k^{il} (where $l = 1 \dots 5$) identified by the most powerful peaks and evaluate the relative amplitudes A_k^{il} and B_k^{il} using a least squares approach. After completing this step, a model of each time series can be represented by the following equation:

$$\text{mod}_k^i(t) = q_k^i + t \times m_k^i + \sum_{l=1}^5 [A_k^{il} \sin(2\pi f_k^{il} \times t) + B_k^{il} \cos(2\pi f_k^{il} \times t)]. \quad (10)$$

The model $\text{mod}_k^i(t)$ represents the motion of the station (i) in the component (k), including both the linear and periodic contributes.

Figure 4 shows the periodograms of all 14 sites, both for GIS and for RIS, and reveals the presence of very similar frequencies for almost all the time series, in particular at the period of 1 year and 6 months. There are also some differences in power, which is not strictly correlated with the amplitude of the signal. Figure 5 shows the models (10) both for GIS and for RIS. This comparison indicates that the amplitude of the models is of only a few millimeters, meaning that it is close to the sensitivity of the GNSS technique. Nevertheless, the signals described are quite different, especially at higher frequencies. Looking at the North component, a different mean velocity is evident for all the sites. Examining the amplitude of the models, there is an evident reduction from GIS to RIS. This reduction has an average value of about 50 % for all the geodetic components, reaching 75 % in some cases, while in a few other cases, it is less than 10 % on the North component. In order

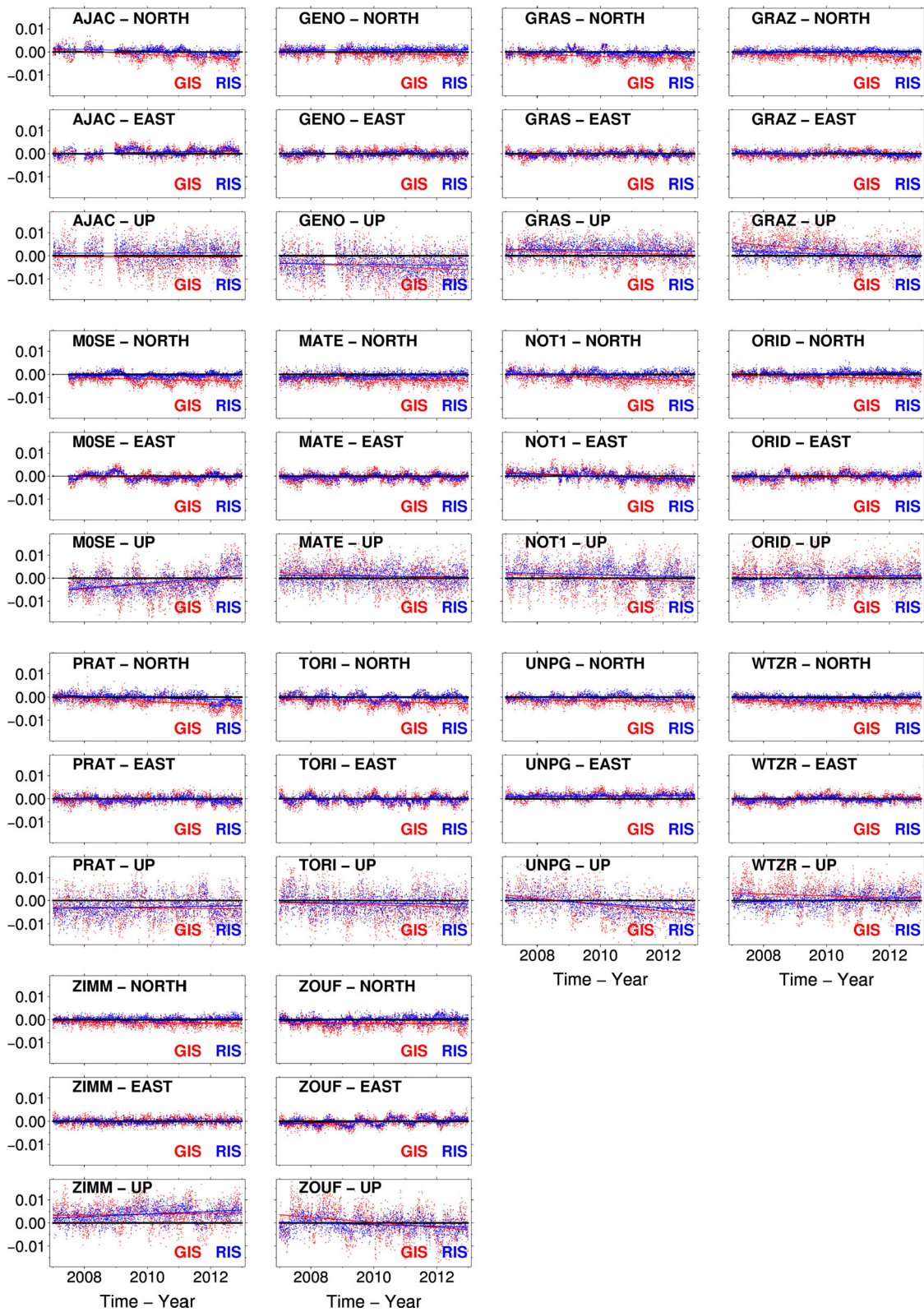


Fig. 3 Δ_k^i time series. The residuals with respect to the EPN_A_IGb08.SNX reference solution are expressed in local geodetic components. X-axis represents the timescale in years, and

Y-axis represents the residuals expressed in meters. Red dots and blue dots refer to GIS and RIS, respectively

Table 2 Repeatability (B_k) and consistency (P_k) calculated for both the GIS and RIS

Site	Repeatability (mm)								Consistency (mm)											
	GIS				RIS				GIS				RIS							
	N	E	Horiz	U	N	E	Horiz	U	N	E	Horiz	U	N	E	Horiz	U				
AJAC	2.0	1.8	2.7	5.3	1.2	1.3	1.8	3.7	-1.3	0.6	1.4	-0.5	0.3	0.7	0.8	1.2				
GENO	1.8	1.6	2.4	5.9	1.1	0.9	1.4	4.1	-0.8	0.0	0.8	-4.4	0.8	0.0	0.8	-3.7				
GRAS	1.9	1.7	2.5	4.1	1.2	0.9	1.5	2.9	-1.9	-0.3	1.9	1.4	-0.3	-0.2	0.4	2.4				
GRAZ	1.5	1.5	2.1	4.9	0.9	0.8	1.2	2.7	-1.6	-0.2	1.6	2.7	0.2	0.0	0.2	0.8				
MOSE	1.8	1.9	2.6	5.4	1.1	1.2	1.6	3.6	-2.2	-0.4	2.2	-2.4	-0.4	-0.2	0.4	-1.9				
MATE	1.8	1.9	2.6	5.1	1.2	1.1	1.6	3.4	-2.2	-0.7	2.3	1.1	-0.6	-0.4	0.7	0.9				
NOT1	1.9	2.4	3.1	6.6	1.2	1.4	1.8	3.9	-1.5	-0.1	1.5	0.1	0.2	-0.1	0.2	1.4				
ORID	1.7	1.9	2.5	5.6	1.1	1.2	1.6	3.0	-1.2	-0.4	1.3	1.3	0.4	0.0	0.4	0.3				
PRAT	2.0	1.8	2.7	5.4	1.5	1.1	1.9	3.9	-1.8	-0.3	1.8	-3.0	-0.2	-0.3	0.3	-2.7				
TORI	2.0	2.1	2.9	5.9	1.5	1.3	2.0	3.7	-1.8	-0.2	1.8	-1.9	-0.3	-0.2	0.4	-1.1				
UNPG	1.6	1.8	2.4	5.3	1.2	0.9	1.5	3.5	-1.7	1.2	2.0	-2.0	0.0	1.3	1.3	-1.5				
WTZR	1.5	1.6	2.2	5.1	1.1	0.9	1.4	2.7	-2.2	-0.2	2.2	2.1	-0.4	-0.1	0.4	0.3				
ZIMM	1.5	1.5	2.1	4.8	1.0	0.9	1.3	2.9	-1.3	0.1	1.3	3.7	0.2	0.0	0.2	3.7				
ZOUF	2.0	1.7	2.6	5.6	1.3	1.3	1.8	3.2	-1.7	-0.2	1.7	0.2	0.0	-0.2	0.2	-0.7				
P_k	1.8	1.8	2.5	5.4	1.2	1.1	1.6	3.4	B_k				1.6	0.4	1.7	1.9	0.3	0.3	0.5	1.6
Impr. from GIS to RIS (%)					34 %	40 %	37 %	37 %	Impr. from GIS to RIS (mm)				1.3	0.1	1.2	0.3				

Columns 2–9 refer to repeatability, and columns 10–17 to consistency. The results are expressed in a local geodetic reference frame (North, East and Up). The North and East component are also combined in a horizontal (Horiz) component. All the results for each site (column 1) are expressed in millimeter. The last two rows report a synthesis in terms of averaged values and relative improvements, respectively

Table 3 Pearson’s correlation coefficients calculated on the v_k^i time series of the WTZR station and each of the others, expressed in the local geodetic components

Site	Correlation coefficient ρ_{rs}					
	GIS			RIS		
	N	E	U	N	E	U
AJAC	0.42	0.46	0.29	-0.09	-0.06	0.11
GENO	0.43	0.59	0.45	-0.17	-0.15	-0.13
GRAS	0.41	0.58	0.38	-0.16	-0.10	-0.03
GRAZ	0.49	0.64	0.57	-0.10	-0.03	-0.16
MOSE	0.43	0.53	0.46	-0.09	0.00	-0.11
MATE	0.38	0.64	0.40	0.10	0.10	-0.05
NOT1	0.37	0.38	0.23	0.18	0.20	0.41
ORID	0.49	0.38	0.40	0.03	-0.20	-0.26
PRAT	0.37	0.57	0.42	-0.14	-0.11	-0.15
TORI	0.38	0.62	0.48	-0.06	0.03	-0.06
UNPG	0.47	0.63	0.46	0.02	0.04	-0.11
ZIMM	0.49	0.51	0.52	0.04	-0.24	-0.04
ZOUF	0.42	0.37	0.55	-0.15	-0.30	-0.24
Average value	0.43	0.53	0.43	-0.05	-0.06	-0.06

Columns 2, 3 and 4 are referred to the GIS, whereas columns 5, 6 and 7 are referred to the RIS

to evaluate the loss of signal resulting from the use of regional transformation parameters instead of global ones, the difference between the GIS and RIS time series was calculated epoch by epoch,

$$d_k^i = v_k^{i-GIS} - v_k^{i-RIS} \tag{11}$$

On this new time series, $mod_k^i(t)$ was estimated using (10). The obtained results are shown in Fig. 6, where all the d_k^i signals are superimposed on the same graphs. This figure shows a high correlation between all the d_k^i series, which demonstrates the presence of a common signal with a magnitude of few millimeters in all 14 stations. This common signal can explain why the Pearson coefficient is higher for GIS than for RIS, as shown in Table 3. The red line in Fig. 6 represents the average signal of the differences between GIS and RIS. The red signal was analyzed using LSP, and especially for the horizontal components, two main frequencies were found in terms of amplitude. These have a period of 1 year and 6 months, respectively. The magnitude (peak to peak) of the recomposed average signal is about 2 mm for the horizontal components and about 5 mm for height.

Having calculated all the signal models, it is possible to recalculate the noise of the time series with respect to their

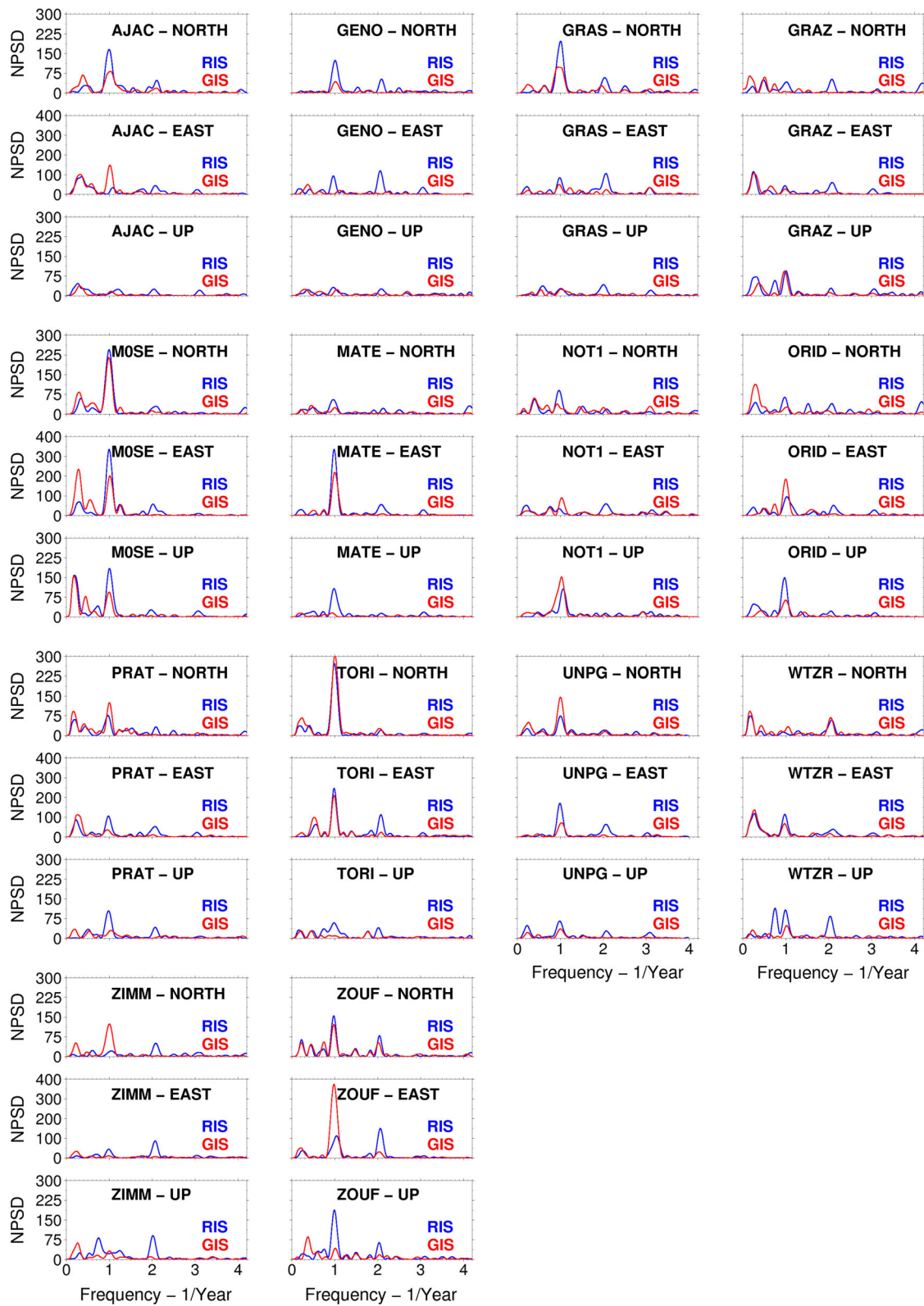


Fig. 4 Comparison of the periodograms obtained from the v_k^i time series for both GIS and RIS. For each site, three periodograms are reported, related to the North, East and Up components. The X-axis

represents the frequency expressed in year⁻¹, whereas on the Y-axis, the normalized spectral power density is reported

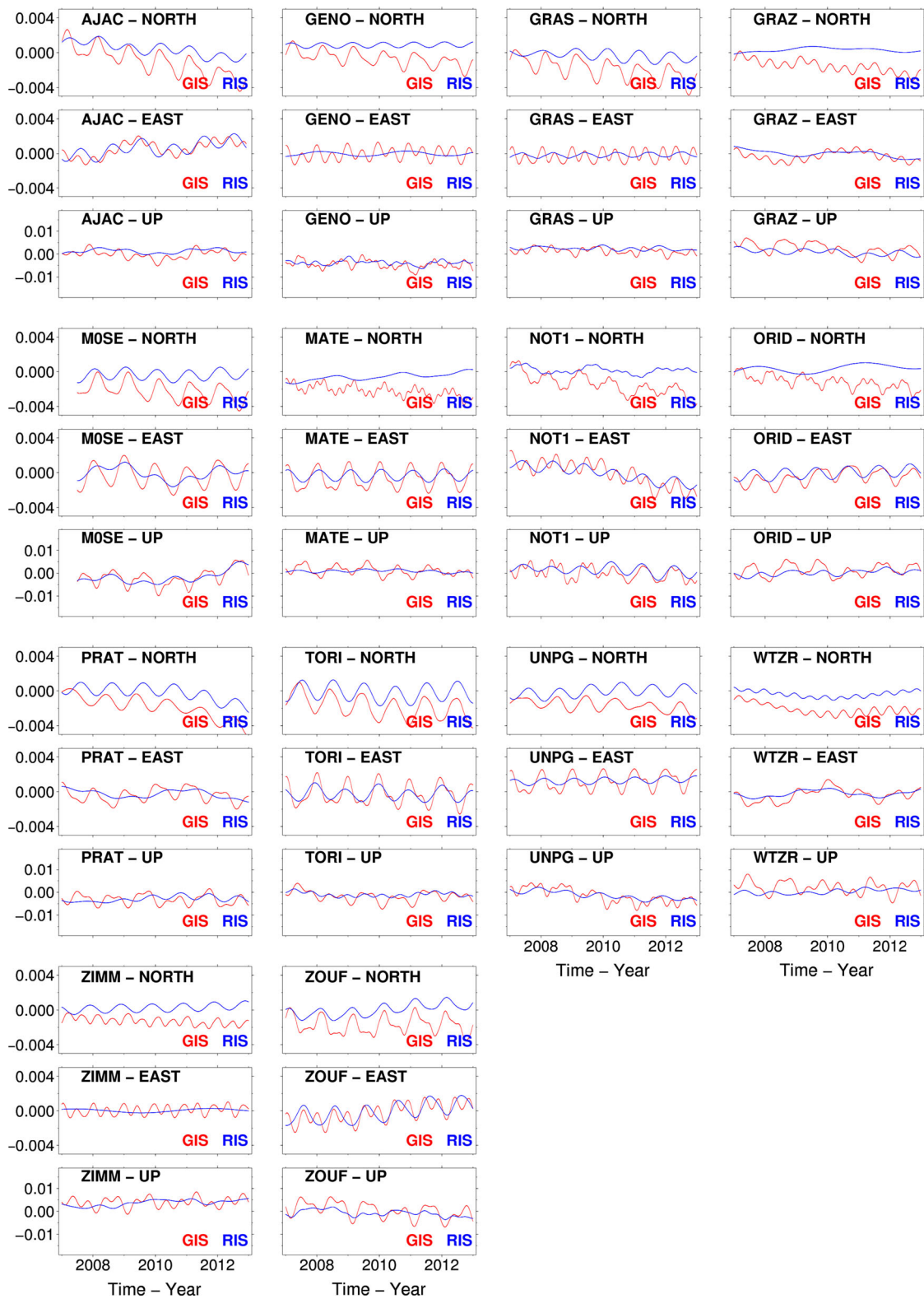
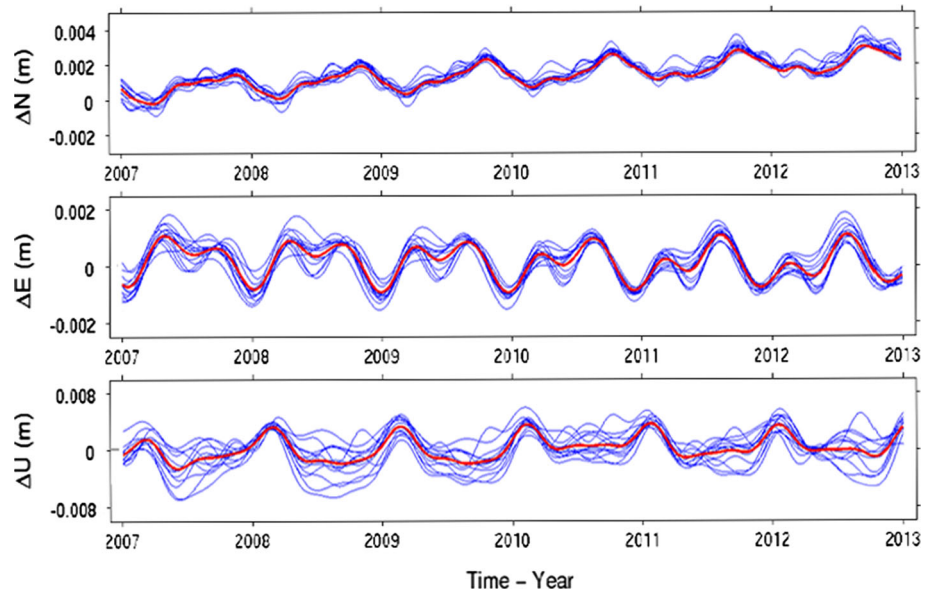


Fig. 5 Representation of the mod_k obtained by means of the first five most powerful frequencies of the Lomb–Scargle periodogram and the linear motion. Red Lines represent the models obtained by GIS,

whereas the blue ones are related to the RIS. All models are referred to a local geodetic reference system, and the values are expressed in meters

Fig. 6 Superimposition of all the models calculated for the d_k^i time series of the residuals between GIS and RIS. Each signal is referred to the local reference frame of the considered site. The *red lines* represent the averaged signals that characterize the whole considered area and have an amplitude of about 2 mm on the North and East component and about 5 mm on the Up



nonlinear model of movement instead of their regression line. To do this, we subtract $mod_k^i(t)$ from the Δ_k^i time series to obtain a new residual time series (w_k^i), which indicates the residual values with respect to the model,

$$w_k^i = \Delta_k^i - mod_k^i(t) \tag{12}$$

The p_k^i coefficients calculated for w_k^i of GIS and RIS (w_k^{i-GIS}, w_k^{i-RIS}) are representative of the residual noise of the time series. Their values are given in Table 4. In particular, the values relating to RIS are 33–38 % lower than for GIS. This result means that the improvement of the repeatability for RIS shown in Table 2 is not only due to the decrease in the amplitude of the signals within the time series. The reduction of noise with respect to the periodical movement of the sites, shown in this test, means that there is an improvement in the precision of the technique used to describe the movements themselves. In other terms, looking at Fig. 6 and Table 4, we can conclude that, if we perform a regional alignment, we can expect to lose a common signal, but the local periodicities are preserved and identified even better, due to the lesser scattering of the w_k^{i-RIS} time series compared to the w_k^{i-GIS} times series.

Nevertheless, global parameters are still very reliable in reducing global biases, such as the instability of earth orientation parameters. However, since these parameters are calculated considering a global network, some local common residual signals cannot be absorbed by the global transformation parameters. When those signals are meaningful at the regional scale, the regional transformation parameters allow for a higher consistency of the estimated coordinates.

Table 4 Precision parameters p_k^i for the residuals w_k^i to the models mod_k^i both for GIS and for RIS

Site	Residual noise to the estimated models					
	GIS (mm)			RIS (mm)		
	N	E	U	N	E	U
AJAC	1.7	1.6	4.9	1.1	1.1	3.6
GENO	1.6	1.4	5.6	1.1	0.9	3.9
GRAS	1.7	1.5	3.9	1.1	0.9	2.8
GRAZ	1.4	1.3	4.3	0.9	0.8	2.5
M0SE	1.4	1.4	4.2	0.9	1.0	3.0
MATE	1.7	1.5	4.7	1.2	0.9	3.3
NOT1	1.8	2.1	5.9	1.2	1.3	3.4
ORID	1.6	1.7	4.9	1.0	1.0	2.8
PRAT	1.8	1.6	4.9	1.3	1.0	3.8
TORI	1.7	1.7	5.3	1.2	1.1	3.6
UNPG	1.5	1.5	4.7	1.0	0.9	3.4
WTZR	1.4	1.4	4.3	1.0	0.8	2.6
ZIMM	1.4	1.4	4.2	0.9	0.9	2.7
ZOUF	1.7	1.5	4.7	1.2	1.0	2.9
Average value	1.6	1.5	4.8	1.1	1.0	3.2
Improvement GIS to RIS (%)				33	38	33

The last two rows report a synthesis in terms of averaged values and relative improvements, respectively

Conclusions

In the present work, a test was performed using GPS data generated over 6 years by 16 permanent stations located in Italy and in neighboring countries. To obtain the daily solutions, RINEX files were calculated using a PPP approach and the GIPSY-OASIS II software. The daily

native solutions were first aligned to the IGS realization of the ITRS by using the official JPL X-files, thus obtaining the Global ITRS Solution (GIS). The same *native* solutions were then aligned to a European densification of the ITRS, applying a set of customized regional transformation parameters and obtaining the Regional ITRS Solution (RIS).

First, the transformation of the *native* solutions into IGB08 using the official JPL X-files led to a reduction of the correlation coefficients between the time series, reaching an average value of about 0.4, which is significantly lower than the correlation coefficient of the previous values, which are between 0.7 and 0.9. Then, by aligning the PPP solutions to the ITRS by using a regionally based set of transformation parameters, it was possible to obtain a stronger reduction of the correlation between the time series, with the coefficients reaching values close to zero. This means that the use of global transformation parameters does not remove a common signal from the sites, but it can be otherwise removed by using regional parameters.

Looking at the applications where there is the need to achieve solutions that are as close as possible to a formally defined reference frame, such as the European densification of IGB08, the repeatability and the consistency of the PPP solutions were evaluated relative to the reference solution. The statistical parameter relating to repeatability has highlighted that the scattering of the RIS time series is reduced by about 37 % compared to GIS. As for consistency, GIS and RIS make it possible to reach a millimeter-level accuracy, but, in this test, where EPN_A_IGb08.SNX has been assumed as the reference, the RIS reaches values of 0.3 mm in plane and 1.6 mm in height, slightly better than the GIS.

The analysis in the frequency domain performed by means of the Lomb–Scargle periodogram shows evidence that almost the same frequencies are present in GIS and RIS. Considering the first five most powerful frequencies, a model of the local movements of all the sites was obtained for the two solutions. The comparison between the GIS and RIS models underlines the fact that there are differences in the amplitude of these signals, which are generally greater for the GIS, especially at the highest frequencies. The residual noise was obtained by subtracting the models from each time series and then evaluated. The noise values for the GIS are generally higher than those of RIS by more than 30 %, where the noise reduction in RIS reaches 38 % for the East component. This noise reduction seems to indicate better precision for the RIS time series, and it follows that a more precise description of the local site movements can be obtained. This result seems to be interesting and will be the subject of further studies aimed at reaching a better

comprehension of the reasons behind this and the characteristics of these different noises. A similar analysis in the frequency domain was performed using the time series of the differences between the GIS and RIS. The models obtained highlight a common signal with a magnitude of about 2 mm in horizontal and 5 mm in height, which is present in almost all the sites and components and is almost eliminated in the RIS.

All of these results should be only slightly different when considering different areas or networks, at least whenever the number of stations used to calculate the regional parameters generates a good level of redundancy for the equations, which, therefore, reduces the dependence of those parameters on the local movements of a single site. We showed that it is possible to improve the PPP performance by carrying out a daily calculation of a regional network, located in the area of the survey and covering a suitable number of stations. If the formal solutions in the desired reference frame are available for each site, it is possible to calculate the daily transformation parameters with a suitable redundancy and apply these to each PPP solution calculated in the area. Despite the necessary efforts to obtain RIS, we will emphasize that the parameters need only to be calculated once for the same area, as long as the parameters and models applied for the geodetic data processing are the same as those used for the surveys, therefore maintaining the strength of the PPP strategy in terms of independence of the solutions. Moreover, the high level of calculation efficiency of the PPP approach means that the regional transformation parameters can be calculated on a daily basis, obtaining the regionally transformed solutions after only a short delay.

Acknowledgments We are grateful to the unknown reviewers for their constructive suggestions and comments that allowed a significant improvement of the paper. We also thank the Generic Mapping Tools (GMT) development team for its useful work.

References

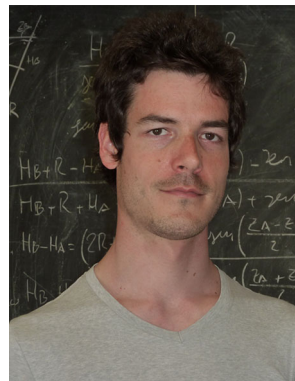
- Altamimi Z, Boucher C (2002) The ITRS and ETRS89 relationship: new results from ITRF2000. In: Torres J, Hornik H (eds) *Mitteilungen des BKG*, vol 10. EUREF, Frankfurt, pp 49–52
- Barbarella M, Gandolfi S, Ricucci L, Zanutta A (2009) The new Italian geodetic reference network (RDN): a comparison of solutions using different software packages. In: *Proceedings of EUREF symposium*, Florence, Italy, 27–30 May
- Bertiger W, Desai SD, Haines B, Harvey M, Moore AW, Owen S, Weiss JO (2010) Single receiver phase ambiguity resolution with GPS data. *J Geod* 84(5):327–337
- Bisnath S, Gao Y (2009) Current state of precise point positioning and future prospects and limitations. In: *Observing our changing earth*. Springer, Berlin, pp 615–623. doi:10.1007/978-3-540-85426-5_71

- Boucher C, Altamimi Z (2011) Memo: specifications for reference frame fixing in the analysis of a EUREF GPS campaign. <http://etrs89.ensg.ign.fr/memo-V8.pdf>
- Bruyninx C, Becker M, Stangl G (2001) Regional densification of the IGS in Europe using the EUREF permanent GPS network (EPN). *Phys Chem Earth, Part A* 26(6):531–538
- Bruyninx C, Altamimi Z, Caporali A, Kenyeres A, Lidberg M, Stangl G, Torres JA (2013) Guidelines for EUREF densifications. ftp://epncb.oma.be/pub/general/Guidelines_for_EUREF_Densification.pdf
- Dong D, Fang P, Bock Y, Cheng MK, Miyazaki S (2002) Anatomy of apparent seasonal variations from GPS-derived site position time series. *J Geophys Res* 107(B4):2075
- Frey Mueller J (2009) Seasonal position variations and regional reference frame realization. In: *Geodetic reference frames*. Springer, Berlin, pp 191–196
- Griffiths J, Ray JR (2009) On the precision and accuracy of IGS orbits. *J Geod* 83(3–4):277–287
- Hurst K (1995) Precise orbital products available from JPL. GIPSY-OASIS II Newsletter. V2N1, 1–3. ftp://sideshow.jpl.nasa.gov/pub/usrs/PS-DOCUMENTS/GOA_newsletter_v2n1.ps
- Kedar S, Hajj GA, Wilson BD, Heflin MB (2003) The effect of the second order GPS ionospheric correction on receiver positions. *Geophys Res Lett* 30(16):1829
- Kouba J (2008) Implementation and testing of the gridded Vienna mapping function 1 (VMF1). *J Geod* 82(4–5):193–205
- Legrand J, Bruyninx C (2009) EPN reference frame alignment: consistency of the station positions. *Bull Geod Geomat* 68:19–34
- Lomb NR (1976) Least-squares frequency analysis of unequally spaced data. *Astrophys Space Sci* 39(2):447–462
- Mao A, Harrison CGA, Dixon TH (1999) Noise in GPS coordinate time series. *J Geophys Res* 104(B2):2797–2816
- Pearson K (1895) Note on regression and inheritance in the case of two parents. *Proc R Soc Lond* 58(347–352):240–242
- Rebischung P, Griffiths J, Ray J, Schmid R, Collilieux X, Garayt B (2011) IGS08: the IGS realization of ITRF2008. *GPS Solut* 16(4):483–494
- Rebischung P (2012) [IGSMail-6663] IGB08: an update on IGS08. <https://igscb.jpl.nasa.gov/pipermail/igsmail/2012/007853.html>
- Scargle JD (1982) Studies in astronomical time series analysis. II—Statistical aspects of spectral analysis of unevenly spaced data. *Astrophys J* 263:835–853
- Völksen C (2005) Stochastic deficiencies using precise point positioning. In: *Proceeding of EUREF symposium of the IAG sub-commission for Europe (EUREF)*. Bratislava, Slovakia, 2–5 June 2004, EUREF Publication No. 14, *Mitteilungen des Bundesamtes für Kartographie und Geodäsie, Band 35*, pp 302–308
- Wang G, Kearns T, Yu J, Saenz G (2014) A stable reference frame for landslide monitoring using GPS in the Puerto Rico and Virgin Islands region *Landslides* 11:119–129
- Webb FH, Zumberge JF (1997) An introduction to GIPSY/OASIS-II. JPL Publication D-11088, Jet Propulsion Lab, Pasadena



monitoring deformation processes of structures and territory.

Stefano Gandolfi received the Degree in Physics (with laude) in 1993 and the Ph.D. in Geodetic and Topographic Sciences from the University of Bologna in 1997. He is currently associate professor of geomatic at the University of Bologna and coordinator for the MSc degree in Environmental Engineering Study Program. His scientific interests are concentrate on the definition and maintenance of regional reference frames and on the use of GNSS data for



Luca Tavasci is a Ph.D. student in the School of Engineering and Architecture at the University of Bologna, Italy. He received the MSc in Civil Engineering at the School of Engineering and Architecture at the University of Bologna, Italy. His current research interests include PPP data processing, the analysis of global or regional reference systems and the analysis of GNSS time series.



creation of automatic procedures for GNSS data processing.

Luca Poluzzi is a Ph.D. student in the School of Engineering and Architecture at the University of Bologna, Italy. He received his MSc in Civil Engineering at the School of Engineering and Architecture at the University of Bologna, Italy. His current research interests include monitoring of structures through GNSS technology, the analysis of GNSS time series, creation of sequential filter to improve the accuracy of the GNSS kinematic time series, creation of automatic procedures for GNSS data processing.